

Delamination and Fracture Modeling Techniques for Shell Composite Structures in LS-DYNA®

Alessandro Polla^{1,2}, Paolo Piana³, Enrico Cestino¹, Giacomo Frulla¹

¹ Department of Mechanical and Aerospace Engineering (DIMEAS), Politecnico di Torino, Torino, Italy;

² Aerospace Engineering and Aviation, RMIT University, Melbourne, Australia;

³ Structural Analysis Expert.

Email: alessandro.polla@polito.it

1 Introduction

Define numerical analysis capable of predicting the behaviors of laminates composites is a research challenge for engineers and scientists from the first implementation of laminated model for shell elements in 1984 [1]. In these last 35 years all aspects of composite materials behavior have been evaluated such as for example, the impact response, crack propagation, crushing resistance. All contributions, for example from Abrate [2], Farley et al. [3], Botkin et al. [4] to actuals individuated a lot of ways to study numerically all aspects associated to related topic, as described and clearly resumed in the following picture.

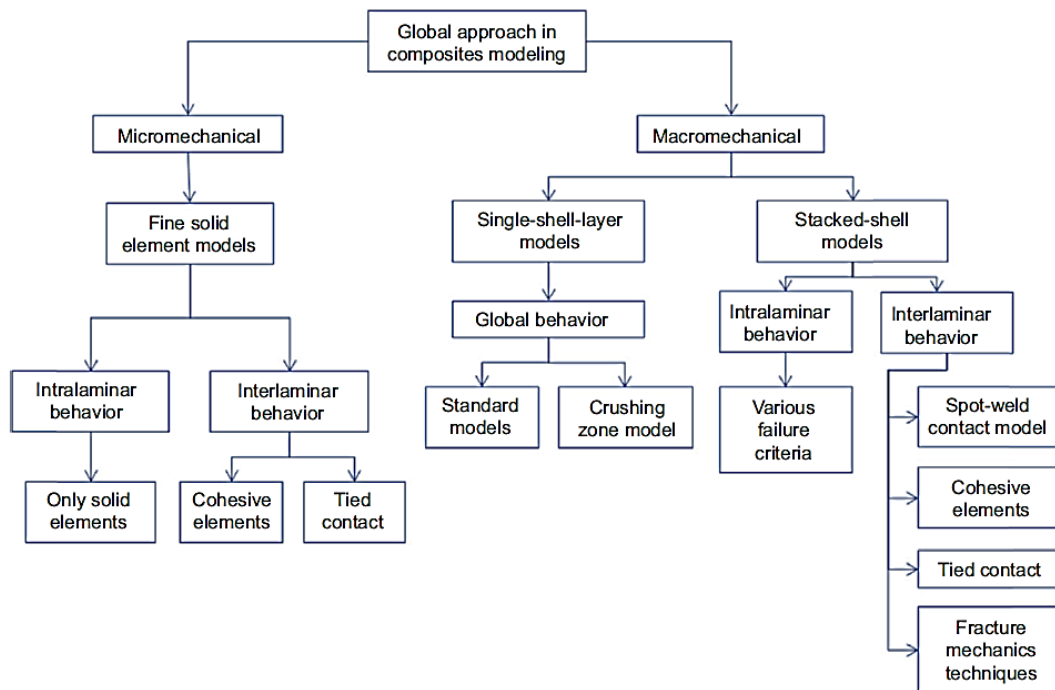


Fig.1: Classification of numerical models for impact on composite laminates [5].

In order to obtain the best correlation with the experimental behavior only the most complex models can be used to characterize the failure behavior of components made by composites. These methodologies strictly focalized results on single specific behavior and they are applicable only with straightly detailed FE model. On the other hand, the methodology belonging to macroscale point of view, typically is selected as the best choice to correlate the structure physical behavior with failure information. Such type of models are characterized by a lot of parameters (up to 70 [6]) where someone are not strictly physical such as described in [7]. Their implementation on a FE model always requires a calibration phase of parameters which involves a lot of time in iterative processes and many resources for experimental tests. Very often the results obtained for the global structure lost the predictable aim that the numerical simulation must have in engineering problems like reported in [7].

In order to maintain the predictive capability of numerical investigation on composite structure, this and future works try to find and clarify constitutive relations between the material models parameters and mechanical material properties. These works will reduce the importance of calibration phase in this type of simulations and open the possibility to obtain results with acceptable correlation levels with experimental test. In particular, the object of this first study is the evaluation and the definition of a relation useful to define the cohesive interface stiffness $ET - EN$ used in all most common models with multi-linear traction-separation laws (MAT_138, MAT_184, MAT_ADD_COHESIVE) [8,9,10].

$$\begin{bmatrix} \sigma_1 \\ \sigma_2 \\ \sigma_3 \end{bmatrix} = \begin{bmatrix} E_T & 0 & 0 \\ 0 & E_T & 0 \\ 0 & 0 & E_N \end{bmatrix} \begin{bmatrix} \delta_1 \\ \delta_2 \\ \delta_3 \end{bmatrix} \quad \left[\frac{N}{mm^2} \right] = \left[\frac{N}{mm^3} \right] [mm]$$

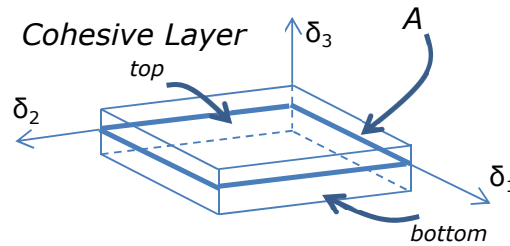


Fig.2: Cohesive element: constitutive equation with stiffness interface matrix and units.

2 Modeling Methodology

Like as described in Fig.1, there are different numerical representation techniques used to accurately reproduce the orthotropic nature of reinforced fiber composite materials.

As reported in the literature [11], for orthotropic composite structures specific technique of representation are necessary depending on which are the goal of numerical representation. For thin-wall composite structures the plane stress hypothesis can be correctly applied. According to this hypothesis, the application of purely two-dimensional models (shells) is therefore correct. Otherwise, for impact load conditions or as a result of transverse loads, the assumptions of plane stress can no longer be verified. In these cases, the implementation of a purely three-dimensional model is recommended. In order to consider the stiffness contribution and damage toughness of a characteristic interlamina present between two adjacent composite plies cohesive elements layer are typically implemented in numerical models. Cohesive elements could be applied in add to solid and shell elements FE meshes to simulate the interlaminar behavior and failure.

The numerical modelling methodology of interest for this work is hybrid technique based on the use of 2D+Cohesive elements. This type of modelling turns out to be ultimately less complex and computationally more performing than complete 3D-based and 3D-Cohesive methodologies.

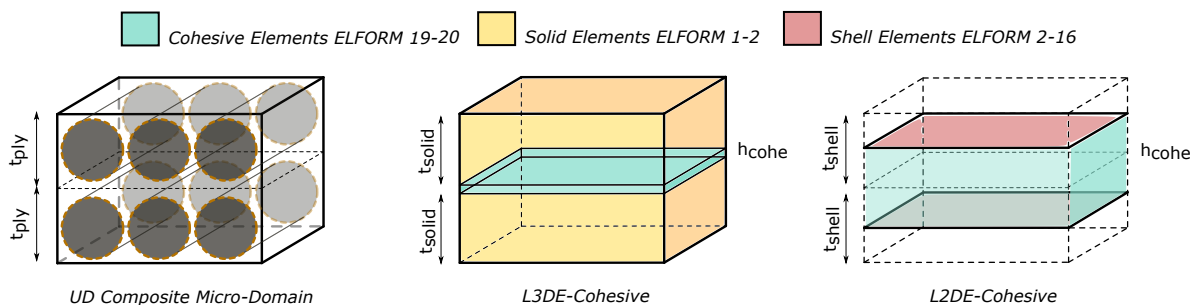


Fig.3: Schematic representation of different FEM-Cohesive models

Let us now introduce the two main numerical modeling techniques which used the cohesive element to describe the interlaminar region and their main characteristics.

Layers of 3D solid Elements – Interlaminar Cohesive Elements (L3DE-Cohesive): each layer which make the laminate is represented by a layer of solid 3D elements. A single ply is connected to the adjacent one by the introduction of a cohesive interlaminar element of zero thickness ($h_{cohe} = 0mm$).

LS-DYNA defines ELFORM 19 solid cohesive formulation for elements utilized with a solid 3D mesh. This modeling practice finds wide application in the industrial and research environment allowing the observation and investigation of the local behavior of the structural component. The main drawback of this method is that it is complex, and it needs lots of computational resources.

Layers of 2D shell Elements – Interlaminar Cohesive Elements (L2DE-Cohesive): single plane of 2D shell elements is imposed for each ply belonging to the laminate. Typically, two-dimensional elements plane of a single ply is placed at the geometric mid-surface of the single layer. To re-establish structural continuity and properly connect the respective ply each other, interlaminar interface elements are commonly inserted node-node. The introduction of cohesive elements restores structural integrity and allows the introduction of transverse stiffness and toughness. LS-DYNA defines ELFORM 20 solid cohesive formulation for the use of two-dimensional mesh with cohesive elements. Compared to the previous case, the cohesive elements will have a not zero thickness ($h_{cohe} = \frac{h_t}{2} + \frac{h_{t+1}}{2} > 0mm$).

2.1 Cohesive Zone Models

CZM tries to represent the mathematical domain which exist around an interlamina region when it fails progressive with a cohesive law. The area underneath the CZM constitutive law defines the energy necessary to propagate the fracture which is commonly associated to the G_c . The more reliable cohesive law is the bi-linear relations. The first segment defines the elastic undamaged region which attributes to the cohesive elements the initial stiffness. The second descending segment on the other hand defines the damage evolution of the cohesive element.

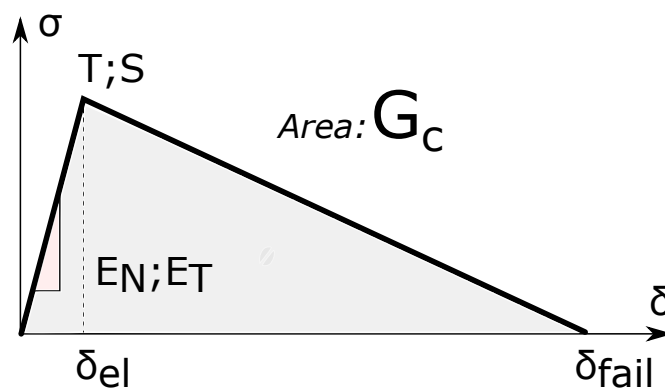


Fig.4: Cohesive Constitutive Law: Bilinear Shape

The cohesive zone model is characterized by three main group of parameters. The first selection which is mainly part of this preliminarily work regards the interface stiffness of the cohesive elements ($E_N; E_T$). The second set of parameters defines the failure stress of the cohesive interlaminar elements ($T; S$). These values perfectly match the local material strength. For composite ply material these quantities reflect the traction strength and the interlaminar shear strength (ILSS).

The last group collects the fracture toughness of the material which constitute the fracture region. The cohesive models request the definition of the specific toughness among every characteristic direction. This set of quantity defines the energy necessary to propagate fracture in mode I, II, III.

The cohesive stiffness could be directly linked to the bulk material and to the technique adopted for the realization of the model. Following will be presented this correlation applied to the MAT_138 cohesive model of LS-DYNA.

3 Cohesive interface stiffness evaluation

From literature an analytical formulation to define the interface stiffness was defined by Turon [12]. That work considers the cohesive elements layers apply to a complete 3D mesh and it is able to define the two-interface stiffness from the mechanical properties of composite material layer in function of a coefficient defined by calibration of experimental results.

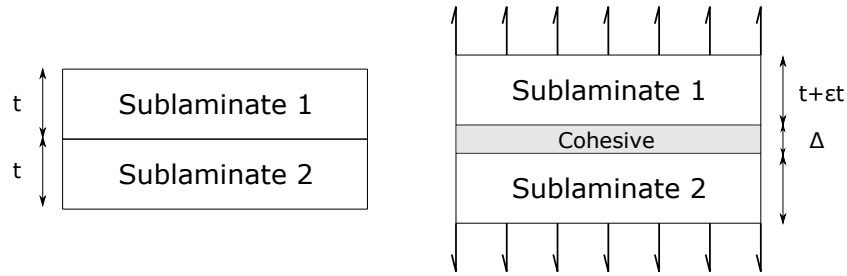


Fig.5: Turon et al. representation to define cohesive interface stiffness

$$E_N = \frac{\alpha E_3}{t} \quad E_T = \frac{\alpha G_{13}}{t} \quad \alpha = 25 \div 50$$

In the last years some other authors proposed some modification to this formulation [13, 14, 15] or they defined similar formulas but all these consider the implementation to complete 3D modelling. The application of these formulas to one L2DE+cohesive model is not considered or reveals some problems. In this case be able to attribute the normal stiffness and the stiffness of the interlaminar resin-rich region that constitutes the real component.

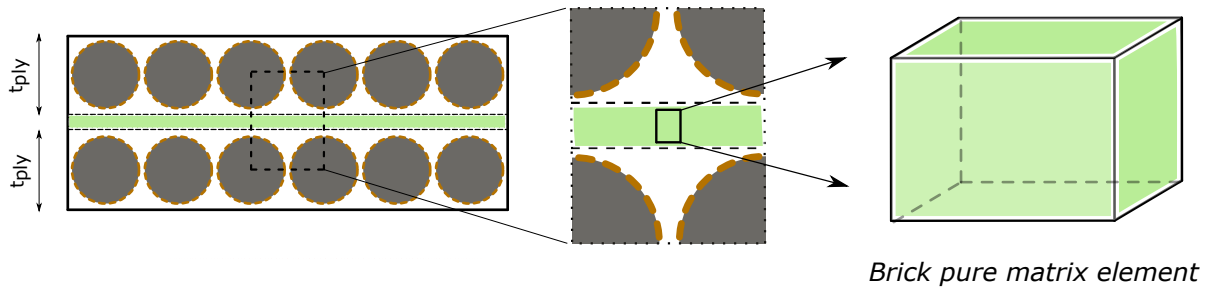


Fig.6: Schematic representation of pure interlaminar matrix region inside a composite material

3.1 Normal Behaviors (MODE I)

The definition of a normal and transverse stiffness is of fundamental importance when are present condition of transversal loads. CZM model therefore provides the definition of a cohesive interface stiffness capable of reproducing the correct local compliance of the structural component. Starting from the definition proposed by Turon et al some hypotheses and observations are now defined to identify a formulation capable of representing the cohesive interface stiffness for L2DE-cohesive models. Let us now proceed by introducing the corresponding hypotheses and analytical observations.

Suppose we have a brick element with a defined planar development (L x L) and a characteristic height h_{el} . In case the element is stressed by a pure form of normal traction (33) the main field of stress that will originate within the brick element will be:

$$\sigma_{33} = E_{33} \epsilon_{33} \quad \epsilon_{33} = \frac{\Delta \delta_{33}}{\delta_{33_0}} = \frac{\delta_{33}}{\delta_{33_0}} = \frac{\delta_{33}}{h_{el}}$$

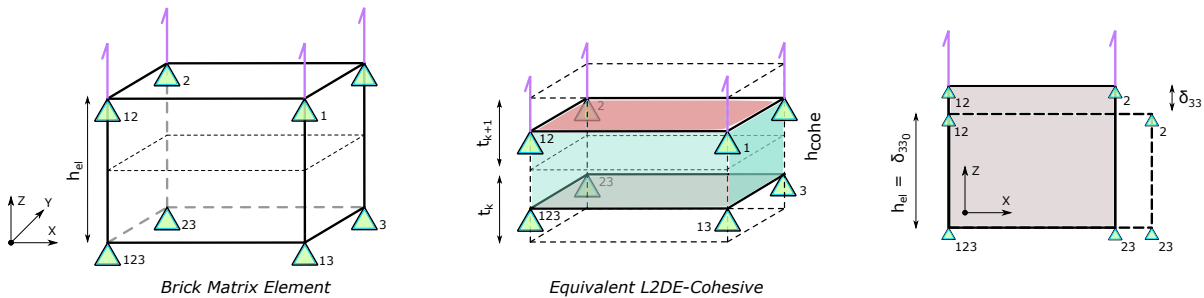


Fig.7: Normal 33 traction load case: Brick 3D Model; L2DE-Cohesive Model; XZ Section View.

For this reason, the formulas can be rewritten considering the following remarks:

$$\sigma_{33} = E_{33} \frac{\delta_{33}}{h_{el}} = \frac{E_{33}}{h_{el}} \delta_{33}$$

Suppose that the brick element seen above is represented by the *L2DE-cohesive* modelling described above. The shell elements thus represented are then connected by a slid element of cohesive material that joins the two mid-surfaces of the individual layers. As observed, it can then define:

$$h_{el} = t_k + t_{k+1}$$

$$\sigma_{33} = \frac{E_{33}}{(t_k + t_{k+1})} \delta_{33} = E_N \delta_{33}$$

In case that two adjacent plies have the same thickness, consequently:

$$t_k = t_{k+1} = t_{ply} = \frac{h_{el}}{2}$$

$$E_N = \frac{E_{33}}{2t_{ply}}$$

It can be therefore demonstrated that the absence of a transverse stiffness in shell elements is consequently schematized and represented by the appropriate selection of the relative thickness with which divide the transverse stiffness of the material E_{33} constituent. The new definition introduced allows the dimensioning of cohesive interface stiffness in normal direction only (33). Taking as reference the mechanical characteristics reported [12] of the matrix direction and consequently characteristics of the interface area between the ply stratified:

$$E_2 = E_3 = 11 \text{ GPa}; \quad \nu_{13} = 0.25; \quad t_k = t_{k+1} = t_{ply} = 0.165 \text{ mm}$$

$$\text{Present approach: } E_N = \frac{E_{33}}{(t_k + t_{k+1})} = \frac{E_{33}}{2t_{ply}} = \frac{11 \text{ GPa}}{2(0.165\text{mm})} = 33.4 \text{ GPa/mm}$$

$$\text{Turon stiffness formula: } E_N = \frac{\alpha E_{33}}{t_k} = \frac{\alpha E_{33}}{t_{ply}} = \frac{50 * 11 \text{ GPa}}{(0.165\text{mm})} = 3334 \frac{\text{GPa}}{\text{mm}}$$

It is immediately observed that the value derived from the current formulation is significantly lower than the transverse stiffness attributable to the formulation of *Turon et al.*

3.2 Shear Behaviors (MODE II & III)

Remember how the cohesive elements can effectively simulate only the stiffness in directions 33, 13, 23. The different membrane stiffnesses are delegated to the two-dimensional FEM elements of the ply. In order to evaluate and analyze the shear behavior the simple shear stress deformation test [16] is applied to the brick element and compared with the relative deformation of the shell-cohesive set. The study begins by analyzing the constitutive relation of the transverse shear that characterizes the observed behavior:

$$\tau_{13} = G_{13} \gamma_{13} \quad \tan(\gamma_{13}) = \frac{\Delta \delta_{11}}{\delta_{33_0}} = \frac{\delta_{11}}{h_{el}}$$

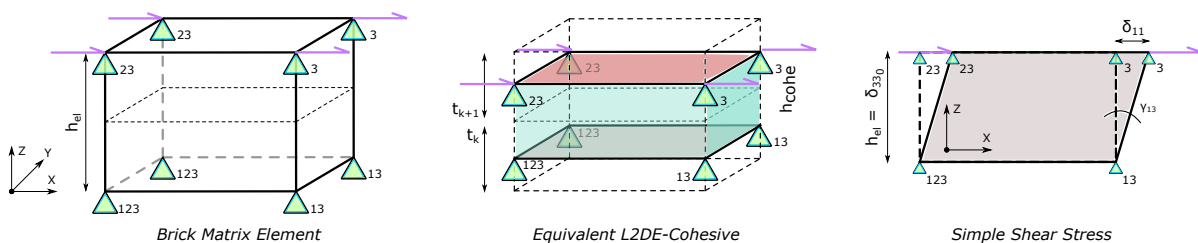


Fig.8: Tangential 13 shear load case: Brick 3D Model; L2DE-Cohesive Model; XZ Section View.

Here the formulation can be rewritten considering some remarks.
It is possible to rewrite the formulation $\text{atan}(x)$ as a series of Maclaurin for $x < |1|$:

$$\tau_{13} = G_{13} \text{atan} \left(\frac{\delta_{11}}{h_{el}} \right)$$

$$\text{atan} \left(\frac{\delta_{11}}{h_{el}} \right) \cong \frac{\delta_{11}}{h_{el}} - \frac{1}{3} \left(\frac{\delta_{11}}{h_{el}} \right)^3 + \frac{1}{5} \left(\frac{\delta_{11}}{h_{el}} \right)^5$$

By replacing the approximate expression within the formulation, it is possible to collect and write:

$$\tau_{13} = G_{13} \left[\frac{\delta_{11}}{h_{el}} - \frac{1}{3} \left(\frac{\delta_{11}}{h_{el}} \right)^3 + \frac{1}{5} \left(\frac{\delta_{11}}{h_{el}} \right)^5 \right] \quad \tau_{13} = \frac{G_{13}}{h_{el}} \left[\delta_{11} - \frac{1}{3} \frac{\delta_{11}^3}{h_{el}^2} + \frac{1}{5} \frac{\delta_{11}^5}{h_{el}^4} \right]$$

Suppose also for this case that the brick element previously seen is represented by the modelling *L2DE-cohesive* previously described. The shell elements thus represented are then connected node-node by a solid element of cohesive material that joins the two mid-surfaces of the individual layers. As observed the hypothesis that can be defined:

$$h_{el} = t_k + t_{k+1}$$

The planar displacement δ_{11} should be considered small enough to define an angular displacement that $\gamma_{13} \rightarrow 0$. Limiting the expansion to linear terms it is therefore possible to reduce the series at the first order and thus obtain the following formulations:

$$\tau_{13} = \frac{G_{13}}{(t_k + t_{k+1})} \delta_{11} = E_T \delta_{11}$$

In case the two adjacent plies have the same thickness, consequently:

$$t_k = t_{k+1} = t_{ply} = \frac{h_{el}}{2}$$

$$E_T = \frac{G_{13}}{2t_{ply}}; E_T = \frac{G_{23}}{2t_{ply}}$$

Taking as reference the mechanical characteristics reported [12] for the matrix direction, consequently the characteristics of the interface area between the ply laminated are:

$$E_2 = E_3 = 11 \text{ GPa}; \quad G_{13} = 4.4 \text{ GPa} \quad \nu_{13} = 0.25; \quad t_k = t_{k+1} = t_{ply} = 0.165 \text{ mm}$$

$$\text{Present approach: } E_T = \frac{G_{13}}{(t_k + t_{k+1})} = \frac{G_{33}}{2t_{ply}} = \frac{11 \text{ GPa}}{2(0.165 \text{ mm})} = 13.4 \text{ GPa/mm}$$

$$\text{Turon stiffness formula: } E_T = \frac{\alpha G_{13}}{t_k} = \frac{\alpha G_{13}}{t_{ply}} = \frac{50 * 4.4 \text{ GPa}}{(0.165 \text{ mm})} = 1334 \text{ GPa/mm}$$

Also for this case it is immediately observed as the value obtained from the current-formulation is remarkably inferior compared to the formulation proposed by *Turon et al.*

4 Modal analysis of composite structure

The evaluation of the modal behavior allows to have a direct and punctual correlation between the structural stiffness and the dynamic behavior of the total structure therefore it's possible to use that to check the validity of new interface stiffness for *L2DE+Cohesive* modelling. Multiple comparisons have been performed between numerical results and experimental values. The literature results were compared with the results obtained using *Turon et al.* stiffness or the present approach definition.

In order to be confident to evaluate the transversal stiffness contributions made by interface stiffness valued calculated, the modal investigations performed are on cylindrical components. In order to perform a modal analysis, LS-DYNA requires the implementation of an implicit model using specific controls and execution keywords [17]. A *PART_COMPOSITE with fully-integrated formulation (ELFORM 16) was used for each ply discretized by *MAT_LAMINATED_COMPOSITE_FABRIC. Interlaminar layers are discretized using cohesive elements with ELFORM 20 and *MAT_COHESIVE_MIXED_MODE or MAT_138.

In elastic modal analysis the main contribution of the selected material model concerns the mass distribution and the definition of its elastic stiffness. For this reason, the contribution related to the toughness and robustness of the material are irrelevant for this analysis.

4.1 Cylindrical Composite Plate: Free Free analysis

The first example concerns a cylindrical plate made of composite material [18]. This is a cylindrical plate with dimensions $a = 200\text{mm}$, $b = 400\text{mm}$ and $h = 2\text{mm}$. The curvature radius of the plates are $R_x = 2000\text{mm}$ and $R_y = +\text{inf}$. The boundary conditions to which the plate is subjected correspond to the free-free case. The laminate has the following stratification [45/-45/45/-45], the individual layers are oriented according to the indicated lamination with respect to the larger side of the plate. The thickness of the single ply is equal to 0.5mm.

The mechanical properties with which the laminate is made up are shown below.

<i>E1</i> [GPa]	<i>E2=E3</i> [GPa]	<i>G12=G13</i> [GPa]	<i>G23</i> [GPa]	<i>v12=v13</i>	<i>v23</i>	<i>RHO</i> [kg/mm ³]
30	2	1	1	0.25	0.45	1.5E-6

The following cohesive properties are useful in order to perform an elastic modal analysis. The values of the cohesive interface stiffness are derived and defined according to the two formulations of this research and previously detailed.

<i>MODE</i>	<i>ROFLG</i>	<i>EN</i> [GPa/mm]	<i>ET</i> [GPa/mm]	<i>RHO</i> [kg/mm ³]
<i>Present Approach formula</i>	1	2	0.8	1.0E-12
<i>Turon stiff, formula ($\alpha = 50$)</i>	1	200	80	1.0E-12

The margin of error for both models with different cohesive interface stiffness formulation does not exceed 5%. The stiffness model proposed by *Turon et al.* alternates underestimated results with overestimated values. Otherwise, the model having the stiffness proposed here typically maintains values underestimated compared to what observed by [18].

Reference Results	Mode 1 [Hz]	Mode 2 [Hz]	Mode 3 [Hz]	Mode 4 [Hz]	Mode 5 [Hz]	Mode 6 [Hz]
Analytical [18]	33,84	53,39	91,30	109,50	111,55	156,92
Turon Stiff	-2.18%	+2.23%	-0.39%	+1.42%	+0.47%	+0.14%
Present Approach	-3.45%	-1.89%	-1.46%	-0.98%	-2.12%	-2.32%

4.2 Elliptic Composite Cylinder: Free Free analysis

The test object of this evaluation involves the construction of a cylinder with elliptical section [19]. The section dimensions of the component are here reported: semi-major axis $a = 2000\text{mm}$, semi-minor axis $b = 1000\text{mm}$, $L = 5000\text{mm}$, $h = 60\text{mm}$.

The component is made of composite material with the following mechanical characteristics and a cross-ply stratification [90/0/90]. The thickness of the single ply is about 20mm. The orientation of the individual ply refers to the main axis of cylinder development.

<i>E1</i> [GPa]	<i>E2=E3</i> [GPa]	<i>G12=G13</i> [GPa]	<i>G23</i> [GPa]	<i>v12=v13</i>	<i>v23</i>	<i>RHO</i> [kg/mm ³]
150	10	5	6	0.25	0.45	1.5E-6

The table containing the mechanical properties attributed to the cohesive material is shown again. Only properties relevant for elastic modal analysis are reported.

MODE	ROFLG	EN [GPa/mm]	ET [GPa/mm]	RHO [kg/mm ³]
Present Approach formula	1	0.25	0.10	1.0E-12
Turon stiff, formula ($\alpha = 50$)	1	25	10	1.0E-12

As can be easily observed below the results obtained by the application of the *Turon et al.* formulation overestimate the frequencies of the component in all the modes analyzed.

Otherwise, the model deriving from the stiffness of current work approximates the modal values of the structure with a remarkably reduced percentage of difference.

Reference Results	Mode 1 [Hz]	Mode 2 [Hz]	Mode 3 [Hz]	Mode 4 [Hz]	Mode 5 [Hz]	Mode 6 [Hz]	Mode 7 [Hz]	Mode 8 [Hz]
Experimental [19]	28,41	28,65	29,54	33,86	79,29	79,46	79,68	79,75
Turon Stiff	+45.44%	+44.42%	+71.29%	+129.56%	+28.67%	+28.61%	+35.54%	+35.55%
Present Approach	-0.45%	-1.25%	+3.04%	+7.94%	-1.57%	-1.45%	-0.81%	-0.71%

4.3 Circular Composite Cylinder: Simple-Simple Supported analysis

The present case concerns a composite cylinder simply supported on both sides [20]. The component has a radius of 1000mm, an overall length of 5000mm and a thickness of 50mm. The stratification used is cross-ply [90/0/90] so the thickness of the single ply is about 16.67mm. The ends of the cylinder are simply supported boundary condition. The properties of the composite and cohesive material used for the numerical model are shown below in tabular form.

E1 [GPa]	E2=E3 [GPa]	G12=G13 [GPa]	G23 [GPa]	v12=v13	v23	RHO [kg/mm ³]
25	1	0.5	0.2	0.25	0.45	1.7E-6

MODE	ROFLG	EN [GPa/mm]	ET [GPa/mm]	RHO [kg/mm ³]
Present Approach formula	1	0.03	0.012	1.0E-12
Turon stiff, formula ($\alpha = 50$)	1	3	1.2	1.0E-12

Reference Results	Mode 1 [Hz]	Mode 2 [Hz]	Mode 3 [Hz]	Mode 4 [Hz]	Mode 5 [Hz]
Analytical [20]	36,98	22,60	23,25	36,62	56,87
Turon Stiff	+0.32%	+178.18%	+384.47%	+343.47%	+272.83%
Present Approach	-0.29%	+2.56%	+3.22%	+1.01%	0%

Similarly, to the above comparison, the results obtained from the model resulting from the *Turon et al.* formulation overestimate the modal values. The formulation presented here, otherwise, defines rigidities congruent with the modeling technique *L2DE-cohesive* selected thus allowing to obtain results with a reduced percentage deviation from what is reported in [20].

5 Fracture mechanics problems: DCB & ENF

In order to complete the validation of the interface stiffness formulas for *L2DE-cohesive* FE model it's necessary investigate the dynamic behavior in terms of stiffness and failures of cohesive interface element defined. Following are reported the comparison between experimental test results and numerical values obtained using the formulas described before and from *Turon et al.* correspondents for DCB and ENF test.

5.1 Double Cantilever Beam: DCB

According to the experimental test procedure ASTM D5528 [21] the DCB numerical test was performed on a laminate consisting of 24-ply unidirectional (0°). The nominal thickness of each ply is 0.165 mm. The specimen was 150-mm-long, 20.0 mm-wide, with two 1.98-mm-thick arms, and it had an initial crack length of 55 mm. Mesh size of all the specimen is 1mm.

Each arm belonging to the test was modeled through the realization of a two-dimensional plane to which was attributed the property of *PART_COMPOSITE. Each part consists of 12 NIP at each of which is

attributed a thickness of 0.165mm. As a result, each NIP is oriented longitudinally to the larger side of the test specimen. The modelling technique *L2DE-cohesive* has also been used for this DCB model.

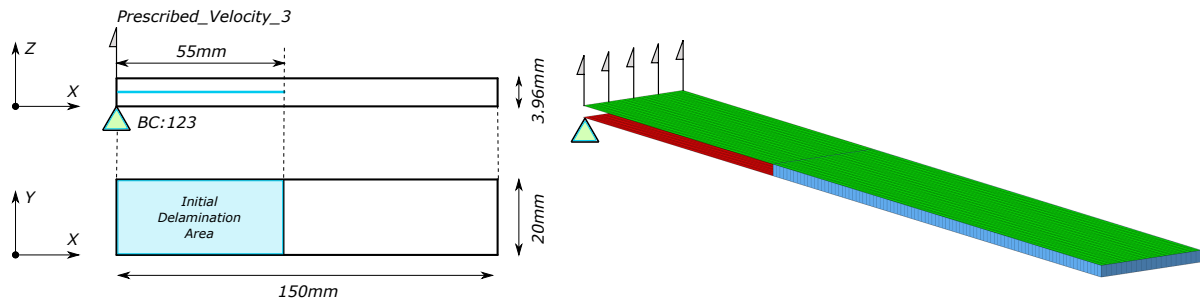


Fig.9: DCB model setting description

The properties of the material T300/977-2 and the cohesive parameter values used in the model are shown below [12, 22].

$E1$ [GPa]	$E2=E3$ [GPa]	$G12=G13$ [GPa]	$G23$ [GPa]	$\nu12=\nu13$	$\nu23$	GIC [GPa*mm]	$GIIC$ [GPa*mm]	T [GPa]	S [GPa]
150	11	6	3.7	0.25	0.45	0.000352	0.00145	0.06	0.08

MODE	INTFAIL	EN [GPa/mm]	ET [GPa/mm]	GIC [GPa*mm]	GIIC [GPa*mm]	T [GPa]	S [GPa]
Present Approach formula	1	33.4	11.25	0.000352	0.00145	0.06	0.08
Turon stiff. formula	1	277.7	111.1	0.000352	0.00145	0.06	0.08

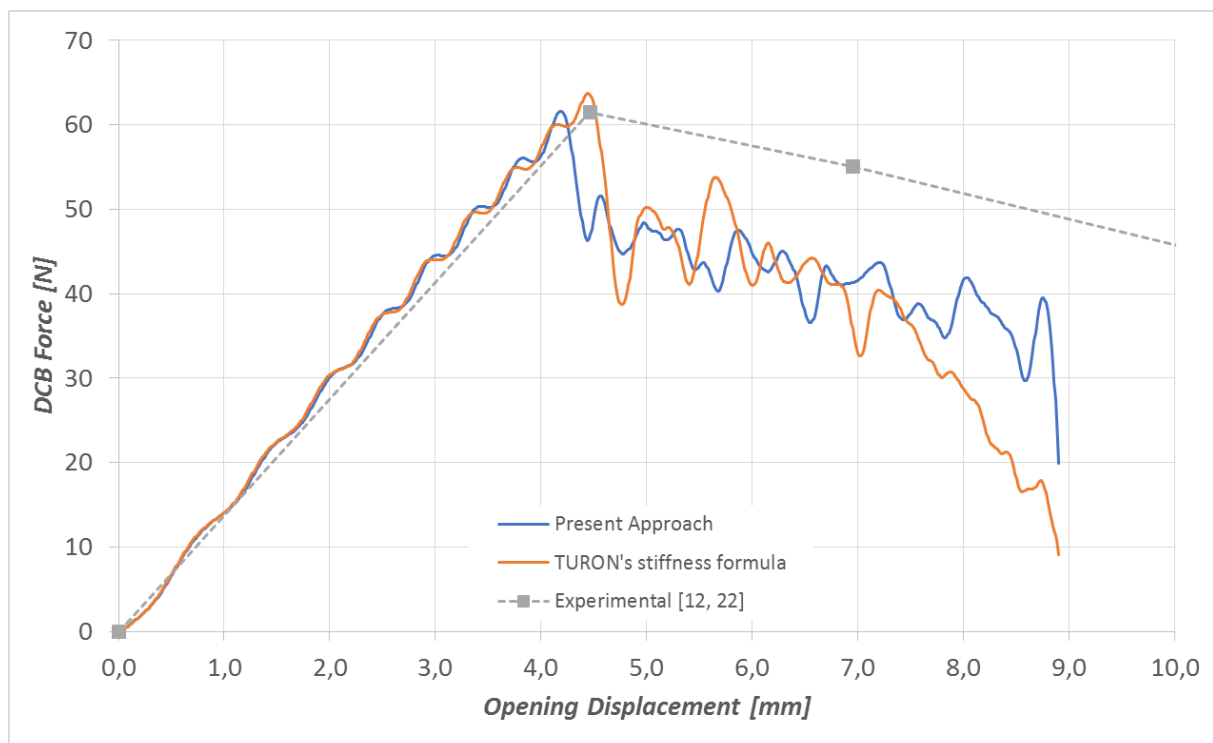


Fig.10: Results comparison for DBC test

To verify the dynamic effect of the cohesive interface stiffness on numerical results, DCB simulation was performed comparing the two different formulations described in this work. Many research have been presented in these years with the adoption of the *Turon et al.* cohesive interface stiffness. The purpose

of this comparison was to verify the accuracy of L2DE-Cohesive modelling technique with the implementation of different cohesive stiffness. The error obtained from using Turon or Present stiffness formulation are perfectly negligible. The observation confirm that the present cohesive stiffness interface formulation could be used also to simulate explicit dynamic problems with the certainty that the Global-Local stiffness of the component is correctly represented.

The linear elastic section of the numerical representations is perfectly comparable to experiment observations. Some differences could be observed in the post-critical behaviour directly linked to the mesh-size and cohesive zone length [12].

Reference Results	Critical Force P [N]	Critical aperture A [mm]
Experimental [12]	61,49	4,46
Turon Stiff	+3.57%	+0.44%
Present Approach	+0.16%	-6%

5.2 End-Notched Flexure: ENF

According to the experimental test procedure ASTM D7905 [23] the ENF numerical test was performed on LS-DYNA R11.1. The test piece analyzed is a laminate consisting of 24-ply unidirectional (0°) in PEEK/APC2 [24]. The nominal thickness of each ply is 0.130 mm. The specimen was 102-mm-long, 25.4 mm-wide, with two 1.56-mm-thick arms, and it had an initial crack length of 39.3 mm. Mesh size of all the specimen is 1mm.

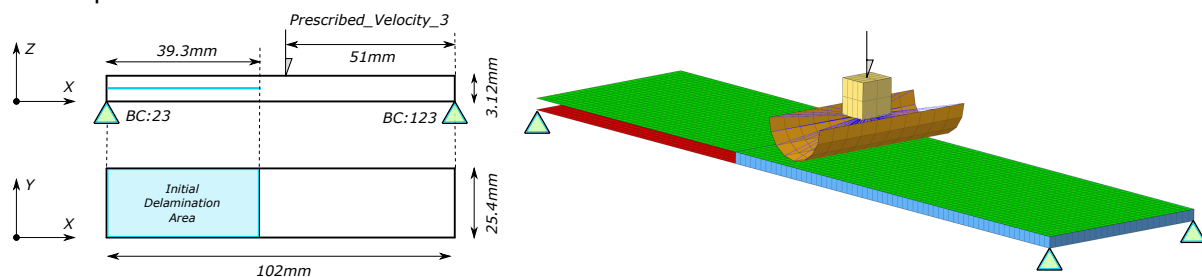


Fig.11: ENF model setting description

This sample was also made using the L2DE-cohesive modeling technique already used in previous models. In this case too, the properties of the PEEK/APC2 material with which the test piece was formed are given below. Similarly, the characteristics attributed to the cohesive material are reported as above.

E1 [GPa]	E2=E3 [GPa]	G12=G13 [GPa]	G23 [GPa]	v12=v13	v23	GIC [GPa*mm]	GIIC [GPa*mm]	T [GPa]	S [GPa]
122.7	10.1	5.5	3.7	0.25	0.45	0.000969	0.001719	0.08	0.1

MODE	INTFAIL	EN [GPa/mm]	ET [GPa/mm]	GIC [GPa*mm]	GIIC [GPa*mm]	T [GPa]	S [GPa]
Present Approach formula	1	26.00	10.00	0.000969	0.001719	0.08	0.1
Turon stiff. formula	1	323.7	129.4	0.000969	0.001719	0.08	0.1

Reference Results	Critical Force P [N]	Critical aperture A [mm]
Experimental [24]	733,96	3,89
Turon Stiff	+6.35%	-0.25%
Present Approach	+5.43%	-1%

The linear elastic section of the numerical representations is perfectly comparable to experiment observations. Some differences could be observed in the post-critical behaviour directly linked to the mesh-size and cohesive zone length.

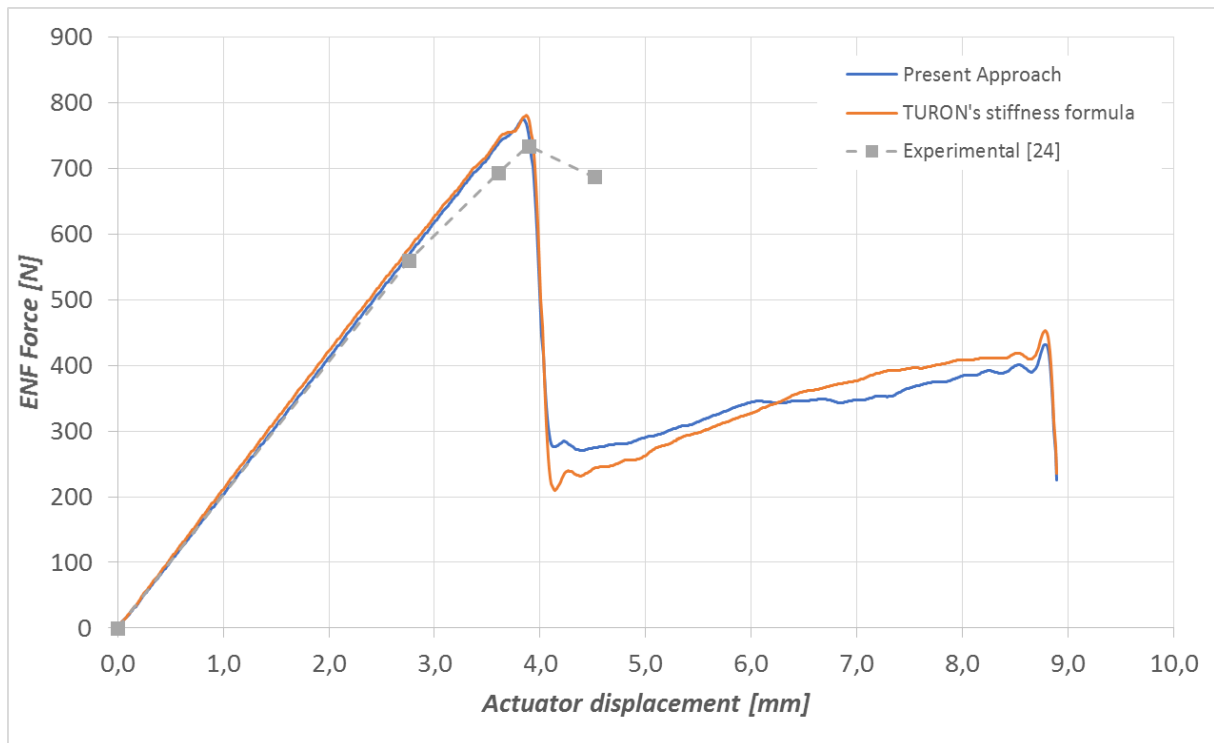


Fig.12: Results comparison for ENF test

6 Conclusions and future applications

The proposed assessments and formulations allow the determination of cohesive interface stiffnesses for L2DE-Cohesive FE application without the use of any calibration phase and without the use of specific experimental tests. The proposed formulation has been validated by making comparisons with implicit and explicit dynamic analysis of finite elements models.

This work initially focused on the analysis of the dynamic behaviour of cylinders with different geometries and radius of curvature for which an experimental reference existed.

The analysis of the results shows that the transverse quantities contribute to the overall stiffness of the component only when the radius of curvature are small and limited. In these respects, the proposed formulation defines percentages better than those achievable by the application of the *Turon et al.* definition. The validation of present approach cohesive stiffnesses was carried out by verifying that the interlaminar fracture behavior of different components was consistent with the experimental observations. For this reason, two reference simulations were used typically for the characterization and calibration of numerical material properties: DCB and ENF tests.

It has been observed that the numerical results of these two specific tests are not strongly influenced by the formulation of cohesive interface stiffness selected. This analogy in the results indicates that the contribution of cohesive stiffness is not strictly significant and that substantial variations of even 100% of the cohesive stiffness value do not change the critical fracture value of both tests in a sensible way.

As described in the literature, progressive rupture behavior is closely influenced by mesh size and cohesive zone length which in the present work have not been examined. Different discourse regards the application of transverse loads or crushing for which, as we will see in subsequent works, the definition of the correct cohesive interface stiffness is necessary and fundamental for the correct reproduction of the physical phenomenon. The aim of present work and future developments will be to define methods and procedures useful for the determination of numerical parameters necessary for the realization of numerical simulations without the parallel experimental calibration of the different properties. The research for this will be expanded with analytical studies on other variables determining the numerical behavior of interlamina and the validation part will be extended to the correlation of more complex scenarios such as low velocity impact and the crushing of structural elements.

7 Literature

- [1] Narayanaswam (Swami), Dr.R: "Layered composite analysis capability for NASTRAN", N85-25968, 1985, COSMIC 13th NASTRAN ® Users' Collq.
- [2] Abrate, S.: "Impact on Composite Structures", Cambridge University Press, 1998.
- [3] Farley, G.L. et al.: "Prediction of the energy absorption capability of composite types", J. Composite Materials, 26, 1992, 338.
- [4] Botkin, M. E. et al.: "Numerical simulation of post-failure dynamic crushing of composite tubes", Proc. Second International LSDYNA3D Conference, 1994.
- [5] Boria, S.: "13 - Lightweight design and crash analysis of composites", Lightweight Composite Structures in Transport, 2016, Woodhead Publishing - Elsevier Ltd., 329-360.
- [6] Pignacca, L.: "Speed and Safety: Composite Materials in Motorsport", Altair EHTC, 2011.
- [7] Feraboli, P. et al: "LS-DYNA MAT54 modeling of the axial crushing of a composite tape sinusoidal specimen", Composites: Part A, 2011, 42: 1809–1825.
- [8] "Keyword user's manual volume II: Material Models LS-DYNA R11", LIVERMORE SOFTWARE TECHNOLOGY CORPORATION (LSTC), 2018.
- [9] The ARUP Campus: "Introduction to Composite Material Modeling in LS-DYNA", ARUP - Oasys Limited 2021.
- [10] Hartman, S. et al.: "Introduction to Composite Material Modeling with LS-DYNA", LIVERMORE SOFTWARE TECHNOLOGY CORPORATION (LSTC), 2018.
- [11] Mufahi S.A. et al: "Investigation of Delamination Modeling Capabilities for Thin Composite Structures in LS-DYNA", 13th International LS-DYNA Users Conference, 2014.
- [12] Turon A. et al: "An engineering solution for mesh size effects in the simulation of delamination using cohesive zone models", Engineering Fracture Mechanics, 2007, 74: 1665–1682.
- [13] Camanho PP et al. "Numerical simulation of mixed-mode progressive delamination in composite materials.", J Compos Mater 2003;37(16):1415–38.
- [14] Daudeville L. et al. "Delamination analysis by damage mechanics. Some applications." Compos Engng 1995;5(1):17–24.
- [15] Zou Z. et al. "Modelling interlaminar and intralaminar damage in filament wound pipes under quasi-static indentation." J Compos Mater 2002;36:477–99.
- [16] Moreira D.C. et al. "Comparison of simple and pure shear for an incompressible isotropic hyperelastic material under large deformation" Polymer Testing 32 (2013) 240–248.
- [17] <https://www.dynaexamples.com/implicit/basic-examples/eigenvalue>
- [18] Ye T. et al. "Free vibration analysis of laminated composite shallow shells with general elastic boundaries", Composite Structures 106 (2013) 470–490.
- [19] Zhao J. et al. "Free vibration analysis of laminated composite elliptic cylinders with general boundary conditions" Composites Part B 158 (2019) 55–66.
- [20] Dongyan S. et al. "Free vibration analysis of laminated composite elliptic cylinders with general boundary conditions" Materials 2020, 13, 884.
- [21] ASTM D5528 "Standard Test Method for Mode I Interlaminar Fracture Toughness of Unidirectional Fiber-Reinforced Polymer Matrix Composites".
- [22] Goyal V. K. et al. "Irreversible constitutive law for modeling the delamination process using interfacial surface discontinue" Composite Structures 65 (2004) 289–305.
- [23] ASTM D7905 "Standard Test Method for Determination of the Mode II Interlaminar Fracture Toughness of Unidirectional Fiber-Reinforced Polymer Matrix Composites".
- [24] Camanho P.P. et al. "Mixed-Mode Decohesion Finite Elements for the Simulation of Delamination in Composite Materials" NASA/TM-2002-211737.